

Determination of the Nucleon-Nucleon Elastic-Scattering Matrix. IV. Comparison of Energy-Dependent and Energy-Independent Phase-Shift Analyses

RICHARD A. ARNDT AND MALCOLM H. MACGREGOR

Lawrence Radiation Laboratory, University of California, Livermore, California

(Received 23 July 1965)

(p,p) and (n,p) scattering data in six energy bands centered at 25, 50, 95, 142, 210, and 330 MeV, have been analyzed. First an energy-dependent analysis was carried out. Then phase-shift energy derivatives were extracted from this analysis and used in carrying out accurate energy-independent analyses. The energy-dependent phase-shift forms were chosen to have a singularity structure consistent with the requirements of partial-wave dispersion equations. A very rapid search procedure was utilized. The isotopic spin-1 scattering matrix was accurately determined over the energy range under consideration. The isotopic spin-0 scattering matrix was also determined, but not to the same accuracy, because of the incompleteness of the (n,p) data selection. The phase-shift analyses were carried out, and the pion-nucleon coupling constant g^2 was determined, using first (p,p) and then (p,p) plus (n,p) data selections. The results were a further substantiation of the charge independence hypothesis. Matrix methods used for the search procedures are discussed, and it is shown how the data normalization constants can be eliminated from the search. A discussion is also included of the use of the inverse error matrix in obtaining quantitative fits with theoretical models.

I. INTRODUCTION

IN papers I to III of this series,¹⁻³ we have published the results of single-energy phase-shift analyses at a set of six energies spanning the elastic-scattering region. In this paper we give the results of analyzing all of these six energies simultaneously, using energy-dependent phase-shift forms that are suggested by dispersion theory. This analysis was done for just (p,p) data, and then for combined (p,p) plus (n,p) data. The data selection was obtained by simply combining the data sets we had used previously.¹⁻³

In the energy-independent analyses,¹⁻³ the data for each analysis spanned a narrow band of energies. Instead of shifting the data so that they would all be at the same energy,^{4,5} we gave the phase shifts an energy dependence by assigning the energy derivatives that we obtained from energy-dependent analyses done by other groups.⁶ Since we now have values for the energy derivatives from the present work, we have used these derivatives to recalculate the single-energy phase shifts. Thus, the energy-independent and energy-dependent analyses form a self-consistent picture, and a comparison of the results gives an accurate evaluation of the merits of the two types of analysis.

In Sec. II we discuss the search procedures used and the functional forms chosen to represent the phase shifts. Section III summarizes the results of the combined (n,p) plus (p,p) analyses. Section IV gives the results of the (p,p) analyses and their bearing on the

question of charge independence. Section V is on the determination of the pion-nucleon coupling constant. Section VI includes a discussion of reduced inverse error matrices and shows how they can be used for potential model fitting. Section VII states our general conclusions.

II. ENERGY-DEPENDENT SEARCH PROCEDURES

In this section we will discuss the method used to minimize the least-squares sum χ^2 , and also the forms used to represent energy-dependent phase shifts.

The search procedure used to minimize χ^2 is based on a linearized second derivative matrix. The basic method has been well known for a long time, but the application to phase-shift analyses was made only recently.⁵ For our final phase-shift values in I-III, we used this type of search. A somewhat modified search procedure was devised by one of us (R. A. A.) and applied to the problem of the energy-dependent analysis. It represents an enormous advantage over the grid-search techniques previously used. Problems that had required hours of computer time with the grid-search method now run in the same number of minutes using the search procedure we describe below.

The least-squares sum χ^2 is defined by the equation

$$\chi^2 = \sum_{i=1}^{N_D} (\alpha^n \theta^i(p) - \theta_{\text{exp}}^i / \Delta \theta_{\text{exp}}^i)^2 + \sum_{j=1}^{N_\alpha} (\alpha^j - 1 / \Delta \alpha_{\text{exp}}^j)^2, \quad (1)$$

where we define $\theta^i(p)$ = observable predicted by the set of parameters p , θ_{exp}^i = observable measured experimentally, $\Delta \theta_{\text{exp}}^i$ = experimental standard deviation, i = observable label, $i = 1 \cdots N_D$, N_D = No. of data points; α^n = normalization parameter, $n = 1 \cdots N_\alpha$, N_α = No. of normalization parameters, $i(n)$ = subset of i that correspond to a parameter n , p = set of parameters specifying the phase shifts, $p = 1 \cdots N_P$, N_P = No. of phase-shift parameters. There are a number of procedures

¹ M. H. MacGregor, R. A. Arndt, and A. A. Dubow, *Phys. Rev.* **135**, B628 (1964).

² M. H. MacGregor and R. A. Arndt, *Phys. Rev.* **139**, B362 (1965).

³ H. P. Noyes, D. S. Bailey, R. A. Arndt, and M. H. MacGregor, *Phys. Rev.* **139**, B380 (1965).

⁴ N. Hoshizaki and W. Watari, *Progr. Theoret. Phys.* (Kyoto) **33**, 337 (1965).

⁵ P. Signell, N. R. Yoder, and N. M. Miskovsky, *Phys. Rev.* **133**, B1495 (1964).

⁶ See Figs. 1 and 2 of Paper II. The energy-dependent analyses were carried out at Yale (Refs. 7 and 8) and at Livermore (Ref. 9).

that can be used to vary the set (p_j, α^n) so as to bring the solution into the vicinity of the χ^2 minimum. We assume that this has been accomplished so that we can use a linear approximation scheme. We write

$$\theta^i(p) \simeq \theta^i(p_0) + \sum_{j=1}^{N_P} \left. \frac{\partial \theta^i}{\partial p_j} \right|_{p_{j0}} \Delta p_j, \quad (2)$$

and

$$\alpha^n \simeq \alpha_0^n + \Delta \alpha^n, \quad (3)$$

where (p_0, α_0) are the values at the true minimum. Then Δp_j and $\Delta \alpha^n$ become the variables of the functional χ^2 , and we will discard all terms higher than first order in these variables. Substituting (2) and (3) in (1),

$$\chi^2 = \sum_i \left[\frac{(\alpha_0^n + \Delta \alpha^n)(\theta^i(p_0) + \sum_k (\partial \theta^i / \partial p_k) \Delta p_k) - \theta_{\text{exp}}^{i-2}}{\Delta \theta_{\text{exp}}^i} + \sum_{j=1}^{N_\alpha} \left(\frac{\alpha_0^j + \Delta \alpha^j - 1}{\Delta \alpha_{\text{exp}}^j} \right)^2 \right]. \quad (4)$$

For a solution we want

$$\partial \chi^2 / \partial \Delta p_j = 0, \quad (5)$$

$$\partial \chi^2 / \partial \Delta \alpha^n = 0. \quad (6)$$

Define

$$\chi_0^i \equiv (\alpha_0^n \theta^i(p_0) - \theta_{\text{exp}}^i / \Delta \theta_{\text{exp}}^i). \quad (7)$$

From (5) we have

$$-\sum_i \chi_0^i \frac{\alpha_0^n}{\Delta \theta_{\text{exp}}^i} \frac{\partial \theta^i}{\partial p_j} = \sum_i \left(\frac{\alpha_0^n}{\Delta \theta_{\text{exp}}^i} \right)^2 \sum_k \frac{\partial \theta^i}{\partial p_j} \frac{\partial \theta^i}{\partial p_k} \Delta p_k + \sum_i \left\{ \frac{\theta^i \alpha_0^n}{(\Delta \theta_{\text{exp}}^i)^2} \frac{\partial \theta^i}{\partial p_j} + \frac{\chi_0^i}{\Delta \theta_{\text{exp}}^i} \frac{\partial \theta^i}{\partial p_j} \right\} \Delta \alpha^n. \quad (8)$$

From (6) we have

$$-\sum_{i(m)} \chi_0^i \frac{\theta^i}{\Delta \theta_{\text{exp}}^i} \frac{(\alpha_0^m - 1)}{(\Delta \alpha_{\text{exp}}^m)^2} = \sum_{i(m)} \left\{ \frac{\alpha_0^m \theta^i}{(\Delta \theta_{\text{exp}}^i)^2} \sum_k \frac{\partial \theta^i}{\partial p_k} + \frac{\chi_0^i}{\Delta \theta_{\text{exp}}^i} \sum_k \frac{\partial \theta^i}{\partial p_k} \right\} \Delta p_k + \sum_{i(m)} \left\{ \left(\frac{\theta^i}{\Delta \theta_{\text{exp}}^i} \right)^2 + \frac{1}{(\Delta \alpha_{\text{exp}}^m)^2} \right\} \Delta \alpha^m. \quad (9)$$

Let

$$A_{jk} = \sum_i (\alpha_0^n / \Delta \theta_{\text{exp}}^i)^2 (\partial \theta^i / \partial p_j) (\partial \theta^i / \partial p_k), \quad (10)$$

$$B_{jn} = \sum_{i(n)} \left(\frac{\alpha_0^n \theta^i}{(\Delta \theta_{\text{exp}}^i)^2} + \frac{\chi_0^i}{\Delta \theta_{\text{exp}}^i} \right) \frac{\partial \theta^i}{\partial p_j}, \quad (11)$$

$$C_{mn} = \delta_{mn} \sum_{i(m)} (\theta^i / \Delta \theta_{\text{exp}}^i)^2 + (1 / \Delta \alpha_{\text{exp}}^m)^2, \quad (12)$$

$$(Y_p)_j = -\sum_i \chi_0^i (\alpha_0^n / \Delta \theta_{\text{exp}}^i) (\partial \theta^i / \partial p_j), \quad (13)$$

$$(Y_\alpha)_m = -\sum_{i(m)} \chi_0^i (\theta^i / \Delta \theta_{\text{exp}}^i) - (\alpha_0^m - 1) / (\Delta \alpha_{\text{exp}}^m)^2. \quad (14)$$

Then Eqs. (8) and (9) become

$$A \Delta p + B \Delta \alpha = Y_p, \quad (15)$$

$$\tilde{B} \Delta p + C \Delta \alpha = Y_\alpha, \quad (16)$$

where \tilde{B} is the transpose of B . Solving,

$$\Delta p = A^{-1} (Y_p - B \Delta \alpha), \quad (17)$$

$$\Delta \alpha = C^{-1} (Y_\alpha - \tilde{B} \Delta p). \quad (18)$$

An important practical simplification can be made here. We can eliminate $\Delta \alpha$ from the equations, giving

$$(A - B C^{-1} \tilde{B}) \Delta p = (Y_p - B C^{-1} Y_\alpha). \quad (19)$$

This means that the normalization parameters do not have to be included explicitly in the search. We can write (15) and (16) as

$$\begin{bmatrix} A & B \\ \tilde{B} & C \end{bmatrix} \begin{bmatrix} \Delta p \\ \Delta \alpha \end{bmatrix} = \begin{bmatrix} Y_p \\ Y_\alpha \end{bmatrix}. \quad (20)$$

Elimination of $\Delta \alpha$ means that we can work with matrices having the dimensionality of A instead of the full dimensionality shown in (20). For the combined analysis, we have used (for example) 58 phase-shift parameters and 48 normalization parameters. Hence the elimination of $\Delta \alpha$ means that we use 58×58 instead of 106×106 matrices for the search.

The search procedure is straightforward. Given a set (p_j, α^n) that are close to (p_{j_0}, α_0^n) , calculate A, B, C, Y_p, Y_α . Then use (19) to recalculate the p_j and use (18) to recalculate the α^n . (Since C is diagonal, the α^n calculation is particularly simple.) A few iterations are enough to ensure convergence.

The search procedure also gives a good approximation to the inverse of the error matrix.⁵ If we define the inverse error matrix as

$$M_{jk} = \frac{1}{2} (\partial^2 \chi^2 / \partial p_j \partial p_k), \quad (21)$$

then by differentiating (1) twice we obtain

$$M_{jk} = A_{jk} + \sum_i \chi_0^i \alpha^n / \Delta \theta_{\text{exp}}^i (\partial^2 \theta^i(p) / \partial p_j \partial p_k). \quad (22)$$

The assumption of linearity says that the second derivative in (22) is small. Hence the matrix A_{jk} is a good approximation to the inverse of the error matrix. In our calculations of M_{jk} , we retained both terms given in (22). In Sec. VI we show how matrix M_{jk} can be modified and used in fitting potential models and other theoretical forms.

The other ingredient necessary for a meaningful energy-dependent phase-shift analysis is a proper parametrization of the phase shifts. The forms chosen must be flexible enough (contain sufficient parameters) that the solution is not "form-limited." Also, we would like to use forms that have some theoretical plausibility. In the Yale energy-dependent analyses,^{7,8} pure mathe-

⁷ G. Breit, M. H. Hull, Jr., K. E. Lassila, K. D. Pyatt, Jr., and H. M. Ruppel, Phys. Rev. 128, 826 (1962).

⁸ M. H. Hull, Jr., K. E. Lassila, H. M. Ruppel, F. A. McDonald, and G. Breit, Phys. Rev. 128, 830 (1962).

mathematical forms were used, and the aim was to obtain solutions that were not form-limited. In the Livermore MIDPOP energy-dependent analyses,⁹ various approximations to dispersion relation discontinuities were tried, but these had only a limited success. These approximations involved treating the left-hand singularities as a sum of poles. An indication of the failure of the forms used for MIDPOP is the fact that the solutions, which were fitted to data in the energy region from 10 to about 380 MeV, gave wild extrapolations at energies just above 400 MeV.¹⁰ One reason for the failure of many of these forms was the fact that the one-pion exchange discontinuity was not explicitly included.

The energy-dependent phase-shift form that we used is

$$\delta_l = \delta_l^{\text{OPEC}}(p_1/g^2) + \sum_{j=2}^N p_j Q_l(\beta_j), \quad (23)$$

where

$$Q_l(\beta_j) \equiv \frac{1}{2}(\mu^2/M(T^2 + 2MT)^{1/2}) \times Q_l[1 + ((\beta_j\mu)^2/MT)], \quad (24)$$

δ_l = partial wave corresponding to orbital angular momentum l , δ_l^{OPEC} = partial wave predicted by the one-pion-exchange-contribution to the potential, N = highest value of j used to represent δ_l , μ = pion rest mass, M = nucleon rest mass, T = nucleon laboratory kinetic energy, Q_l = associated Legendre function of the second kind, $\beta_j = 2, 3, 5, 9$ for $j = 2, 3, 4, 5$, g^2 = pion-nucleon coupling constant.

The parameter p_1 was treated as a free parameter for some of the lowest- l partial waves. For the rest of the partial waves, p_1 was set equal to g^2 . Thus the higher partial waves contain the one-pion discontinuity as the leading term when we view (23) as an expansion in the left-hand discontinuities associated with a partial-wave Mandelstam representation. The Q functions have singularities that coincide with the Mandelstam $2\pi, 3\pi, 5\pi$, and 9π discontinuities when defined with arguments as shown in (24). Thus (23) is an expansion that approximates the singularity structure as given by the Mandelstam representation. In particular, the phase-shift form (23) exhibits the proper T^l threshold behavior.¹¹

The form for 3S_1 was slightly different than shown in (23) since we imposed the requirement that the 3S_1 phase shift approach 180° at zero energy.

III. COMBINED (p,p) PLUS (n,p) PHASE-SHIFT ANALYSES

If we assume that charge independence is valid, then an analysis of (p,p) and (n,p) data together gives both the isotopic spin-zero ($T=0$) and isotopic spin-one ($T=1$) phase shifts. If the (p,p) data are analyzed

⁹ M. J. Moravcsik, H. P. Noyes, H. P. Stapp, and R. Wright (unpublished).

¹⁰ For examples, see Figs. 34–47 in *The Two-Nucleon Interaction* by M. J. Moravcsik (Clarendon Press, Oxford, England, 1963).

¹¹ M. H. MacGregor, Phys. Rev. Letters 12, 403 (1964).

TABLE I. Data selection for the phase-shift analyses. The number of each kind of data is listed.^a

Kind of data	σ	P	D	R	R'	A	C_{NN}	C_{KP}	Total	Com- bined total	
Energy band (MeV)											
				(p,p) data							
25	24	2		3			3			32	
50	20	3	1	5			5	1	1	36	
95	14	28	5	5	4					56	
142	21	55	15	14	10		12			127	
210	7	14	7	7	4		5			44	
310	35	14	6	6			3	3	1	68	
				(n,p) data							
									Total	363	
25	23	6								29	
50	23	15								38	
95	49	47								96	
142	50	28	5	5			5			93	
210	20	6	5							31	
310	35	19								54	
									Total	341	
										704	

^a References 1–3, 13, 14 and Table II describe all of the data listed here.

separately, then just the $T=1$ phase shifts are obtained. It is by now well established that, at least for the experiments we are considering, charge independence is a valid concept.^{1–3,12} It is also our conclusion^{1–3} that the $T=1$ phase shifts obtained from a combined analysis are generally more accurate than those obtained from a separate (p,p) analysis. Indeed, if the (n,p) data are of comparable accuracy to the (p,p) data, this is the expected result, since a larger data selection should lead to more accurate phase shifts. Thus we feel that the results we present in this section represent the most accurate values for the phase shifts that we can obtain from the existing nucleon-nucleon data.

We first carried out an energy-dependent phase-shift analysis, using the phase-shift energy-dependent forms given in (23), and using the matrix search procedure described in the preceding section. The data selection that was used is summarized in Table I. This essentially is the same data collection that was used previously,^{1–3} and the references are given in I–III. The most notable change was the addition of additional (p,p) C_{NN} and C_{KP} measurements at 310 MeV.¹³ Data changes from the previous analyses (I–III) are listed in Table II.

Several choices for the number of free parameters to represent the phase shifts were investigated. For the $T=1$ phases, it was found after some experimentation that 35 free parameters gave the best results. These are listed in Table III. The choice for the proper number of $T=0$ phases to use is more difficult to determine. Three different choices are shown in Table III. The 29-parameter choice is what we would select if we went strictly according to the results of the energy-independent analyses.^{1–3} The 31-parameter choice corresponds to giving the same freedom to the $T=0$ phases

¹² G. Breit, Rev. Mod. Phys. 34, 766 (1962).

¹³ Yu. M. Kazarinov, F. Lehar, G. Peter, A. F. Pisarev, and K. M. Fahp'brukh, Zh. Eksperim. i Teor. Fiz. 47, 848 (1964) [English transl.: Soviet Phys.—JETP 20, 565 (1965)].

TABLE II. Additions and changes to the data selections listed in Papers I-III of this series. In our analyses, we have included (p,p) and (n,p) data in six energy bands spanning the elastic energy region—25 and 50 MeV (Tables I and III of Paper III), 140 MeV (Table XI of Paper I), and 95, 210, and 310 MeV (Tables I, IV, and VI of Paper II). In the present paper we have updated these data selections to include recent additions and changes. These changes are all listed here for the benefit of other workers in the field. We have not included data lying outside the listed energy bands, and we have not included some data within the energy bands that seemed to us to be either redundant or incorrect. In our opinion the data included in the present table and in the tables listed above contain the essential physical content of the nucleon-nucleon scattering experiments between 20 and 350 MeV that have been carried out to date. Inclusion of other data points would not substantially improve our knowledge of the elastic-scattering matrix in this energy region. We do feel that some data disagreements exist and that more complete and more accurate data will be forthcoming in the next few years, particularly with regard to the (n,p) system.

Energy (MeV)	Type of data	$\theta_{c.m.}$ (degrees)	Datum ^a	Normali- zation error	Energy (MeV)	Type of data	$\theta_{c.m.}$ (degrees)	Datum ^a	Normali- zation error
27.4	$(p,p) P(\theta)^b$	45	0.0028±0.0041	0.03	99	$(n,p) \sigma(\theta)^e$	7	11.25±0.50	0.017
27.5	$(n,p) \sigma(\theta)^c$	7	28.5±1.3		14	9.93±0.53			
		14	28.5±1.5		21	8.01±0.50			
		21	29.6±1.8		31	8.63±0.50			
		31	28.3±1.6		41	6.46±0.45			
		41	27.5±1.9		51	5.21±0.32			
		51	27.3±2.0		62	4.56±0.38			
		62	26.5±2.1		72	4.25±0.32			
		72	27.0±2.1		82	3.65±0.34			
		159	25.3±1.6		92	3.69±0.28			
		166	26.8±1.6	102	4.48±0.46				
		173	29.9±1.9	112	3.96±0.46				
50	$(p,p) D(\theta)^d$	70	-0.241±0.075	0.017	122	4.92±0.66	0.038		
51.7	$(p,p) P(\theta)^b$	60	0.0364±0.0091		78	2.14±0.76			
53.2	$(p,p) P(\theta)^b$	75	0.0075±0.0077		88	2.90±0.64			
52.5	$(n,p) \sigma(\theta)^e$	7	18.36±0.77		98	4.21±0.56			
		14	18.02±0.90		108	5.06±0.30			
		21	18.18±1.05		118	5.85±0.30			
		31	14.89±0.74		129	6.74±0.38			
		41	14.16±0.92		139	7.52±0.40			
		51	12.91±0.79		149	9.50±0.63			
		62	12.36±0.90		159	9.76±0.57			
		72	10.98±0.74	166	11.84±0.68				
		82	10.88±0.90	173	12.63±0.77				
		92	10.36±0.78	90	$(n,p) P(\theta)^e$	21.5	17.8±4.2	0.051	
		102	9.50±0.92	31.5	30.5±4.6				
		112	11.12±1.15	41.5	31.1±4.2				
		78	11.60±1.24	51.5	37.0±4.1				
		88	12.61±1.15	61.5	38.3±5.6				
		98	11.38±1.03	71.5	35.2±3.2				
		105	11.64±0.59	81.5	27.4±5.2				
		118	12.20±0.59	91.5	13.7±9.3				
		129	12.04±0.63	101.5	14.2±4.3				
		139	12.91±0.68	98.5	22.8±3.6				
		149	14.83±0.88	108.5	13.9±1.9				
		159	14.99±0.93	118.5	8.0±2.0				
		166	17.80±0.98	128.5	2.5±1.7				
		173	17.01±1.07	138.5	-0.3±1.7				
50	$(n,p) P(\theta)^e$	21.5	10.7±2.7	0.048	148.5	-2.0±1.9	0.073		
		31.0	15.0±2.6		158.5	1.2±2.3			
		41.0	17.6±2.3		21.5	18.0±6.2			
		51.0	20.9±2.1		31.5	31.3±6.8			
		61.0	23.2±3.3		41.5	46.5±7.0			
		71.0	20.0±1.8		51.5	46.4±6.5			
		81.0	20.6±2.5		61.5	40.3±7.7			
		91.0	18.8±3.0		71.5	44.0±5.4			
		101.0	13.5±2.5		81.5	46.0±8.6			
		99.0	19.5±2.6		91.5	26.6±15.0			
		109.0	10.5±1.2	101.5	15.5±7.5				
		119.0	8.2±1.2	98.5	23.3±5.7				
		129.0	6.2±1.0	108.5	14.3±3.1				
		139.0	4.3±1.0	118.5	5.5±3.2				
		158.5	0.7±1.4	128.5	4.1±2.7				
98	$(p,p) P(\theta)^f$	31.3	-0.22±0.11	0.024	138.5	-0.8±2.7	0.024		
98	$(p,p) R(\theta)^g$	41.6	-0.40±0.10		148.5	-0.4±2.9			
		51.7	-0.39±0.09		158.5	-7.8±3.7			
		61.9	-0.12±0.13		147	$(p,p) P(\theta)^h$		72.0	-0.151±0.055
		72.0	-0.18±0.20		140	$(p,p) R(\theta)^i$		82.1	-0.047±0.080
		31.6	0.59±0.23		142	$(p,p) P(\theta)^f$		41.0	0.491±0.037
98	$(p,p) R'(\theta)^g$	41.9	0.66±0.18		143	$(n,p) P(\theta)^j$		51.0	0.491±0.019
		52.0	0.70±0.18					62.0	0.446±0.018
		62.6	0.52±0.30						

TABLE II. (continued).

Energy (MeV)	Type of data	$\theta_{c.m.}$ (degrees)	Datum ^a	Normali- zation error	Energy (MeV)	Type of data	$\theta_{c.m.}$ (degrees)	Datum ^a	Normali- zation error
		72.0	0.366±0.021				32.3	0.378±0.022	
		82.5	0.211±0.022				42.9	0.379±0.013	
		92.5	0.104±0.017				53.4	0.303±0.021	
		108.0	0.014±0.015				63.9	0.251±0.025	
213	$(p,p) R'(\theta)^k$	118.0	-0.019±0.015				76.2	0.142±0.024	
		30	0.490±0.032				89.4	-0.005±0.016	
		40	0.390±0.028		315	$(p,p) C_{NN}(\theta)^n$	45	0.90±0.51	
		50	0.177±0.024		315	$(p,p) C_{KP}(\theta)^n$	45	0.74±0.51	
345	$(p,p) \sigma(\theta)^l$				300	$(n,p) \sigma(\theta)^i$	75	2.02±0.20	
315	$(p,p) P(\theta)^m$	21.6	0.305±0.019	0.04	350	$(n,p) \sigma(\theta)^o$	160.7	6.02±0.07	0.03

^a We list only the data that are different from our previous listings.
^b See Ref. 4 of Paper III.
^c J. P. Scanlon, G. H. Stafford, J. J. Thresher, P. H. Bowen, and A. Langford, Nucl. Phys. 41, 401 (1963).
^d T. C. Griffith, D. C. Imrie, G. J. Lush, A. J. Metheringham, and P. D. Wroath, Rutherford Laboratory PLA Progress Report, 1963 (unpublished).
^e Polarization is expressed in percent. These data supersede the values quoted from Ref. 13 in Paper II and Ref. 16 in Paper III. The present values are from Harwell report AERE-R4973, 1965 (unpublished) by Langford *et al.* which has been submitted for publication (private communication from A. Langford to P. Signell).
^f These data should be multiplied by 0.911 in accordance with Ref. 4 of Paper III. Since we used no normalization restraint, this is merely a formal change and does not affect the results of the analyses.
^g O. N. Jarvis, B. Rose, C. F. Cox, and G. H. Eaton, Nucl. Phys. 61, 194 (1965). These data were included in the final 95-MeV analyses in Paper III (see the addendum) but were not listed in the data table.
^h These data should be multiplied by 0.933 in accordance with Ref. 4 of Paper III. This change was incorporated in the results of Paper II.
ⁱ This is a publication error that was not caught in the galley proofs.
^j References 31 and 34 of Paper I. These data have been multiplied by

0.933 in accordance with Ref. 4 of Paper III. These changes were incorporated in the results of Paper II.
^k These data are based on Refs. 20 and 21 of Paper II. These are the data that were actually used in the final 210-MeV analyses described in Paper II. The $R'(\theta)$ values shown in Table IV of Paper II were preliminary ones, and they should have been replaced by the values listed here.
^l The last six data points constitute a separate run and should be normalized separately, with a normalization error that is also 0.05.
^m The errors listed in Table VI of Paper IV include the normalization error. The present listing has this normalization error removed to give the correct relative errors.
ⁿ Reference 13.
^o The data at this energy were actually taken in two separate runs. The experimenters adjusted the runs by using a theoretical form. Examination of our results shows that their form was essentially equivalent to ours for the purpose of normalization. Hence it was not necessary for us to normalize the two runs separately. The over-all normalization of 3% was arrived at by the experimenters, using an interpolation procedure. We have tried using this normalization and also letting the data float freely. We found that the normalization constraint is essential to achieve consistent results between the EDA and EIA.

that we have awarded to the $T=1$ phases. The 23-parameter choice maintains this freedom in the *number* of non-OPEC phases, but it requires the phases to have a smoother non-OPEC variation, which keeps them somewhat closer to their OPEC values.

When we tried a combined-analysis problem using 64 parameters (Table III), we found that the phases were quite strongly affected by the values we adopted for g^2 . This indicated to us that we should free as many $T=0$ phases as $T=1$ phases, since a strong g^2 dependence means that we have not allowed enough non-OPEC freedom in the phases. We then tried a 66-parameter analysis. However, the phase shifts now exhibited both a strong g^2 dependence and rather wild deviations from OPEC in the higher l phases. The relative paucity of (n,p) data precludes our using this much freedom in the $T=0$ phases. Hence as a compromise between the 64- and 66-parameter results, we chose 58 free parameters, as listed in Table III. This gives some freedom to the full range of $T=0$ phase shifts, but it requires the higher partial waves to maintain a rather smooth energy dependence. The 58-parameter set showed only small phase-shift changes with variations in g^2 . The χ^2 values for the 64-, 66-, and 58-parameter solutions were 655, 649, and 662, respectively. Hence all three choices give fits to the data that are statistically essentially equivalent. However, we feel that the $T=0$ phase shifts corresponding to the 58-parameter set are the most meaningful ones from a physical point of view. It is our opinion that these $T=0$ phases represent the best values that can be obtained from the existing nucleon-

nucleon data by using the modified phase-shift analysis. The $T=1$ phase shifts showed a remarkable stability in that they were virtually unaffected either by changes in g^2 or by the choice of 64, 66, or 58 free parameters for the combined analysis. This is a reflection of the completeness of the (p,p) data selection.

TABLE III. Number of free parameters used to represent the energy-dependent phase shifts. The parameters are defined in Eq. (23) of the text.

$T=1$ phases			$T=0$ phases			
1S_0	5 ^a	4 ^a	3S_1	5 ^{a,b}	4 ^{a,b}	4 ^{a,b}
3P_0	5 ^a	5 ^a	1P_1	3 ^a	3 ^a	3 ^a
3P_1	3	2	ϵ_1	4 ^a	4 ^a	3 ^a
3P_2	3	3	3D_1	3	3	2
1D_2	3	2	3D_2	3	3	2
ϵ_2	3	3	3D_3	3	3	2
3F_2	2	1	1F_3	2	2	1
3F_3	2	1	ϵ_3	2	2	1
3F_4	2	1	3G_3	2	2	1
1G_4	2	1	3G_4	2	2	1
ϵ_4	2	1	3G_5	...	1	1
3H_4	1	...	1H_5	...	1	1
3H_5	1	...	ϵ_5	...	1	1
3H_6	1	...				
Total	35	24 ^c		29	31	23
Combined total				64	66	58

^a The free parameter p_1 is included.
^b The phase shift is modified to approach 180° at zero energy.
^c In an effort to see how few phase-shift parameters we could get by with, we did a computer calculation in which the least important parameters were removed one at a time from the search. The value for χ^2 was 299 for 35 parameters. The value for 24 parameters was 321. The phase shifts for the 24-parameter solution are not as reliable as for the 35-parameter solution. In particular, 3F_2 for the 24-parameter solution continues to rise at high energies, giving a behavior that is not consistent with results at 660 MeV. In reducing from 35 to 24 parameters, 3H_4 was the first (smallest deviation from OPEC) phase removed, and 3H_5 was the last.

TABLE IV. Comparison of χ^2 values for energy-dependent and energy-independent phase-shift analyses. These values are for 35 $T=1$ and 23 $T=0$ phase-shift parameters, 363 (p,p) and 341 (n,p) data points, and a g^2 value of 13.

Energy band (MeV)	Energy-dependent analyses				Energy-independent analyses			
	(p,p)	(p,p) plus (n,p)		(p,p)	(p,p) plus (n,p)		χ^2 Total	
	$\chi^2(p,p)$	$\chi^2(p,p)$	$\chi^2(n,p)$	$\chi^2(p,p)$	$\chi^2(p,p)$	$\chi^2(n,p)$		
25	21	25	17	42	16	17	12	29
50	32	36	28	64	22	22	18	40
95	43	43	101	144	38	39	97	136
142	111	109	130	239	102	112	101	213
210	34	35	45	80	28	28	25	53
330	58	58	35	93	53	54	27	81
Total χ^2	299	306	356	662	259	272	280	552

Table IV gives a summary of χ^2 values from the various analyses. Since the combined analysis used 704 data points and 58 free parameters, the expected χ^2 is 646. The χ^2 we obtained for the energy-dependent analysis was 662. When the six energies were analyzed separately, as described below, the separate χ^2 sums added up to a value of 552. Hence this "rock-bottom" value of 552 is the best that any energy-dependent analysis should in principle hope to attain. The difference between 662 and 552 can be attributed to two causes: (1), the form [Eq. (23)] we have chosen is not flexible enough; (2) the data sets are not completely consistent with each other. (We should point out here that a χ^2 value of 662 represents an excellent fit to the data, and the difference between 552 and 662 is not large from a practical standpoint.) To investigate the flexibility of our phase-shift forms, we tried several combinations of free parameters other than the ones listed in Table III. It was found that if more freedom is

put into the higher partial waves, they have a tendency to develop unphysical wiggles. The 1S_0 phase does require five free parameters, as does 3P_0 . Adding more free parameters in the search would not substantially lower the χ^2 values of Table IV. We conclude that the difference between 552 and 662 is due principally to small inconsistencies among the various data sets. This is discussed in more detail below.

Having completed the combined (p,p) plus (n,p) energy-dependent phase-shift analysis, we obtained phase-shift energy derivatives at each of the six energies and then used these values to recalculate the single-energy analyses.¹⁻³ Thus we are using the same data in both analyses and our phase-shift energy variations are consistent. Comparison of the results enables us to estimate the consistency of the data in the whole energy range. The χ^2 values for the single-energy analyses are listed in Table IV together with the energy-dependent values.

TABLE V. Phase-shift values from the combined (p,p) plus (n,p) energy-dependent analysis, with 58 free parameters and a g^2 value of 13

Energy (MeV)	1S_0	1D_2	1G_4	3P_0	3P_1	3P_2	ϵ_2	3F_2	3F_3	3F_4	ϵ_4	3H_4	3H_5	3H_6
24	49.71	0.70	0.04	7.00	-4.23	2.23	-0.83	0.10	-0.22	0.03	-0.04	0.00	-0.01	0.00
32	45.97	1.02	0.07	9.47	-5.42	3.29	-1.18	0.18	-0.37	0.06	-0.08	0.01	-0.03	0.00
40	42.47	1.35	0.11	11.18	-6.52	4.36	-1.49	0.27	-0.52	0.10	-0.13	0.02	-0.05	0.01
48	39.31	1.67	0.15	12.20	-7.58	5.42	-1.76	0.36	-0.68	0.15	-0.18	0.03	-0.08	0.01
56	36.47	1.99	0.20	12.67	-8.58	6.43	-2.00	0.45	-0.85	0.20	-0.24	0.04	-0.11	0.01
64	33.91	2.30	0.25	12.73	-9.55	7.39	-2.20	0.54	-1.00	0.27	-0.29	0.05	-0.15	0.02
80	29.40	2.90	0.35	12.00	-11.38	9.13	-2.50	0.70	-1.30	0.41	-0.41	0.09	-0.23	0.04
96	25.50	3.47	0.45	10.64	-13.08	10.63	-2.71	0.85	-1.57	0.58	-0.51	0.13	-0.32	0.06
112	22.04	4.02	0.55	9.01	-14.66	11.90	-2.84	0.97	-1.81	0.75	-0.61	0.17	-0.42	0.09
128	18.88	4.54	0.64	7.32	-16.14	12.96	-2.91	1.07	-2.03	0.94	-0.70	0.23	-0.52	0.11
144	15.94	5.04	0.73	5.65	-17.51	13.83	-2.95	1.14	-2.21	1.13	-0.77	0.28	-0.63	0.15
160	13.20	5.53	0.82	4.04	-18.79	14.54	-2.96	1.19	-2.38	1.33	-0.83	0.34	-0.74	0.18
176	10.60	5.99	0.90	2.48	-19.98	15.10	-2.95	1.22	-2.52	1.53	-0.88	0.40	-0.85	0.22
192	8.13	6.43	0.97	0.98	-21.10	15.55	-2.93	1.24	-2.64	1.73	-0.92	0.46	-0.96	0.26
208	5.77	6.86	1.04	-0.50	-22.16	15.88	-2.91	1.24	-2.74	1.93	-0.95	0.52	-1.07	0.30
224	3.51	7.27	1.10	-1.97	-23.15	16.12	-2.89	1.22	-2.83	2.12	-0.96	0.59	-1.18	0.34
240	1.34	7.67	1.16	-3.46	-24.08	16.28	-2.86	1.19	-2.91	2.32	-0.97	0.65	-1.29	0.38
256	-0.75	8.06	1.22	-4.99	-24.97	16.38	-2.84	1.16	-2.98	2.51	-0.96	0.72	-1.40	0.42
272	-2.76	8.43	1.27	-6.56	-25.80	16.41	-2.83	1.11	-3.03	2.70	-0.95	0.78	-1.51	0.47
288	-4.70	8.78	1.31	-8.20	-26.60	16.39	-2.82	1.06	-3.08	2.88	-0.93	0.84	-1.62	0.51
304	-6.58	9.13	1.35	-9.92	-27.35	16.33	-2.82	1.00	-3.11	3.07	-0.91	0.91	-1.72	0.55
320	-8.39	9.46	1.39	-11.73	-28.07	16.23	-2.82	0.94	-3.14	3.24	-0.87	0.97	-1.83	0.59
336	-10.14	9.79	1.42	-13.62	-28.76	16.10	-2.83	0.87	-3.17	3.42	-0.84	1.03	-1.93	0.64
352	-11.83	10.10	1.45	-15.62	-29.42	15.94	-2.85	0.80	-3.19	3.59	-0.79	1.10	-2.03	0.68
368	-13.46	10.40	1.48	-17.71	-30.05	15.76	-2.88	0.72	-3.20	3.76	-0.74	1.16	-2.13	0.72
384	-15.04	10.70	1.50	-19.90	-30.65	15.56	-2.91	0.65	-3.21	3.92	-0.69	1.22	-2.22	0.76
400	-16.58	10.98	1.53	-22.20	-31.23	15.33	-2.95	0.57	-3.22	4.09	-0.64	1.28	-2.32	0.80

TABLE V. (continued).

Energy (MeV)	1P_1	1F_3	1H_5	3S_1	ϵ_1	3D_1	3D_2	3D_3	ϵ_3	3G_3	3G_4	3G_5	ϵ_5
24	-0.39	-0.38	-0.03	78.95	5.35	-2.29	4.07	0.27	0.50	-0.05	0.15	-0.00	0.03
32	-1.12	-0.60	-0.06	73.69	4.92	-3.44	6.02	0.44	0.81	-0.10	0.29	-0.01	0.07
40	-2.07	-0.82	-0.10	68.74	4.25	-4.60	7.91	0.63	1.14	-0.16	0.45	-0.01	0.12
48	-3.17	-1.02	-0.15	64.15	3.53	-5.74	9.69	0.82	1.47	-0.23	0.63	-0.01	0.19
56	-4.39	-1.22	-0.20	59.91	2.86	-6.83	11.34	1.02	1.80	-0.31	0.83	-0.01	0.26
64	-5.68	-1.40	-0.25	55.99	2.29	-7.87	12.85	1.21	2.11	-0.39	1.03	-0.01	0.33
80	-8.38	-1.71	-0.37	49.00	1.47	-9.79	15.42	1.58	2.70	-0.57	1.45	0.00	0.50
96	-11.13	-1.97	-0.48	42.95	1.11	-11.51	17.48	1.91	3.25	-0.76	1.86	0.02	0.67
112	-13.83	-2.19	-0.59	37.68	1.16	-13.05	19.08	2.19	3.76	-0.96	2.27	0.04	0.85
128	-16.45	-2.37	-0.69	33.04	1.53	-14.43	20.31	2.44	4.22	-1.15	2.67	0.08	1.03
144	-18.45	-2.52	-0.78	28.92	2.18	-15.68	21.22	2.64	4.65	-1.35	3.05	0.11	1.20
160	-21.33	-2.65	-0.87	25.24	3.06	-16.80	21.88	2.81	5.05	-1.54	3.42	0.15	1.37
176	-23.58	-2.76	-0.95	21.94	4.11	-17.83	22.33	2.95	5.43	-1.73	3.78	0.20	1.54
192	-25.70	-2.85	-1.03	18.96	5.31	-18.77	22.62	3.06	5.78	-1.92	4.12	0.24	1.70
208	-27.69	-2.92	-1.09	16.25	6.62	-19.63	22.76	3.14	6.11	-2.10	4.45	0.29	1.86
224	-29.57	-2.99	-1.16	13.79	8.02	-20.43	22.79	3.20	6.41	-2.28	4.77	0.33	2.01
240	-31.33	-3.04	-1.22	11.54	9.50	-21.18	22.73	3.24	6.71	-2.46	5.08	0.38	2.16
256	-32.99	-3.09	-1.27	9.47	11.03	-21.87	22.59	3.27	6.99	-2.63	5.37	0.42	2.31
272	-34.55	-3.12	-1.32	7.57	12.60	-22.52	22.40	3.27	7.25	-2.80	5.66	0.46	2.45
288	-36.02	-3.16	-1.36	5.81	14.21	-23.13	22.15	3.27	7.50	-2.96	5.93	0.51	2.58
304	-37.39	-3.18	-1.40	4.19	15.84	-23.71	21.87	3.25	7.74	-3.12	6.20	0.55	2.71
320	-38.69	-3.20	-1.44	2.68	17.50	-24.26	21.56	3.22	7.97	-3.28	6.46	0.59	2.84
336	-39.91	-3.22	-1.48	1.29	19.16	-24.78	21.23	3.18	8.19	-3.43	6.71	0.63	2.96
352	-41.05	-3.23	-1.51	-0.02	20.83	-25.28	20.88	3.13	8.40	-3.59	6.95	0.66	3.08
368	-42.13	-3.24	-1.54	-1.23	22.50	-25.75	20.51	3.07	8.60	-3.73	7.19	0.70	3.20
384	-43.15	-3.25	-1.56	-2.36	24.17	-26.21	20.14	3.01	8.80	-3.88	7.41	0.73	3.31
400	-44.11	-3.25	-1.59	-3.42	25.83	-26.64	19.76	2.94	8.99	-4.02	7.64	0.76	3.42

The final phase-shift values from our energy-dependent analysis (EDA) are listed in Table V. We do not quote phase shifts below 24 MeV, since our data selection did not extend to the lower energies. Similarly, quoted phase-shift values above 350 MeV are extrapolations based on our choice (23) for the phase-shift parametrization. The final phase-shift values from the energy-independent analysis (EIA) are listed in Table VI. These values are very close to the values cited in our earlier publications,^{2,3} and they supersede those

based on our choice (23) for the phase-shift parametrization. The final phase-shift values from the energy-independent analysis (EIA) are listed in Table VI. These values are very close to the values cited in our earlier publications,^{2,3} and they supersede those

TABLE VI. Phase-shift values from the combined (p, p) plus (n, p) energy-independent analysis, with phase-shift energy derivatives taken from Table V, and with $g^2=13$. These values supersede our previously published values.^a

	25 MeV	50 MeV	95 MeV	142 MeV	210 MeV	330 MeV
1S_0	49.94±0.41	37.50±0.78	26.33±2.37	16.44±0.74	5.18±0.57	-9.26± 1.56
1D_2	0.62±0.14	2.16±0.27	3.48±0.33	4.90±0.27	7.02±0.32	9.22± 0.67
1G_4				0.63±0.13	1.04±0.16	1.53± 0.33
3P_0	5.80±0.86	12.08±0.79	13.22±1.85	6.44±0.58	-0.79±0.61	-13.21± 1.53
3P_1	-3.55±0.42	-7.98±0.31	-12.78±0.47	-16.99±0.43	-21.59±0.60	-28.87± 1.09
3P_2	2.04±0.16	6.06±0.20	10.18±0.45	13.68±0.22	15.89±0.27	16.18± 0.63
ϵ_2	-0.74±0.35	-2.27±0.36	-2.67±0.36	-2.88±0.16	-2.78±0.19	-3.05± 0.48
3F_2	0.25±0.16	0.55±0.32	0.64±0.59	0.68±0.32	1.58±0.34	0.67± 0.67
3F_3		-0.45±0.41	-1.18±0.67	-2.16±0.22	-2.58±0.21	-3.23± 0.62
3F_4		0.21±0.17	0.48±0.20	0.89±0.18	2.32±0.20	2.93± 0.39
ϵ_4				-0.67±0.07	-0.94±0.09	-0.83± 0.29
3H_4				0.44±0.18	0.47±0.36	1.46± 0.40
3H_5				-0.63±0.17	-0.64±0.22	-2.11± 0.52
3H_6				0.25±0.11	0.41±0.27	0.90± 0.26
1P_1	0.19±1.26	-4.28±1.85	-13.90±3.28	-15.58±2.14	-23.37±8.01	-27.16±13.47
1F_3				-0.92±0.77	-5.53±2.78	-5.83± 5.5
1H_5						-1.6 ± 1.16
3S_1	76.61±6.00	62.15±3.92	44.47±1.85	29.58±0.97	18.23±3.10	-10.32± 9.03
ϵ_1	7.09±1.80	12.77±4.16	0.28±1.67	0.99±0.93	3.13±2.87	28.12± 5.34
3D_1	-2.64±0.30	-7.32±2.37	-10.95±0.78	-15.14±0.74	-22.98±4.04	-20.10± 2.98
3D_2		10.31±3.51	14.95±2.60	23.79±1.20	23.39±4.33	20.49± 4.00
3D_3		-0.37±1.44	1.98±0.65	1.10±0.82	2.82±1.66	3.95± 2.08
ϵ_3				3.31±0.59	7.09±0.96	5.11± 3.52
3G_3				-2.01±0.55	-0.42±1.50	-7.19± 3.54
3G_4				4.18±0.83	4.40±2.60	9.15± 3.36
3G_5				0.13±0.32	0.00±1.50	-0.32± 1.40
ϵ_5						3.10± 1.26

^a See Refs. 1-3.

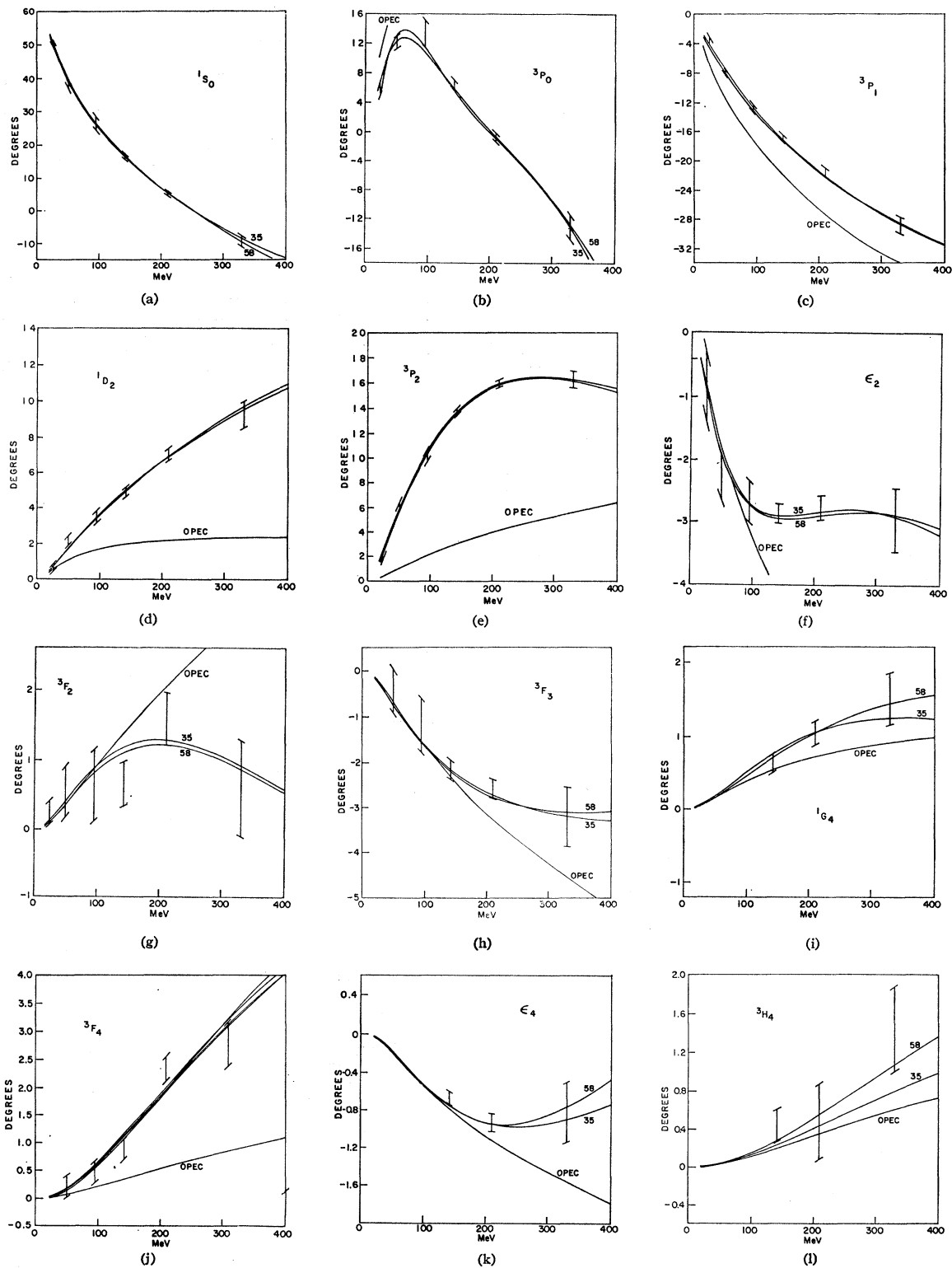


FIG. 1. Energy-dependent phase-shift solutions for 35 and 58 parameters, with $\xi^2=13$. Also shown is the OPEC phase shift and the combined EIA phases. The slope on the error bar shows the slope that was used for the EIA at each energy. The similarity of the $T=1$ phases for the (p,p) (35-parameter) and (p,p) plus (n,p) (58-parameter) solutions illustrates the validity of the charge-independence hypothesis. The deviations from OPEC for some of the higher phases (e.g., ϵ_4 and 3G_4) can also be observed. The labeling on the curves follows their description here.

(continued on next page.)

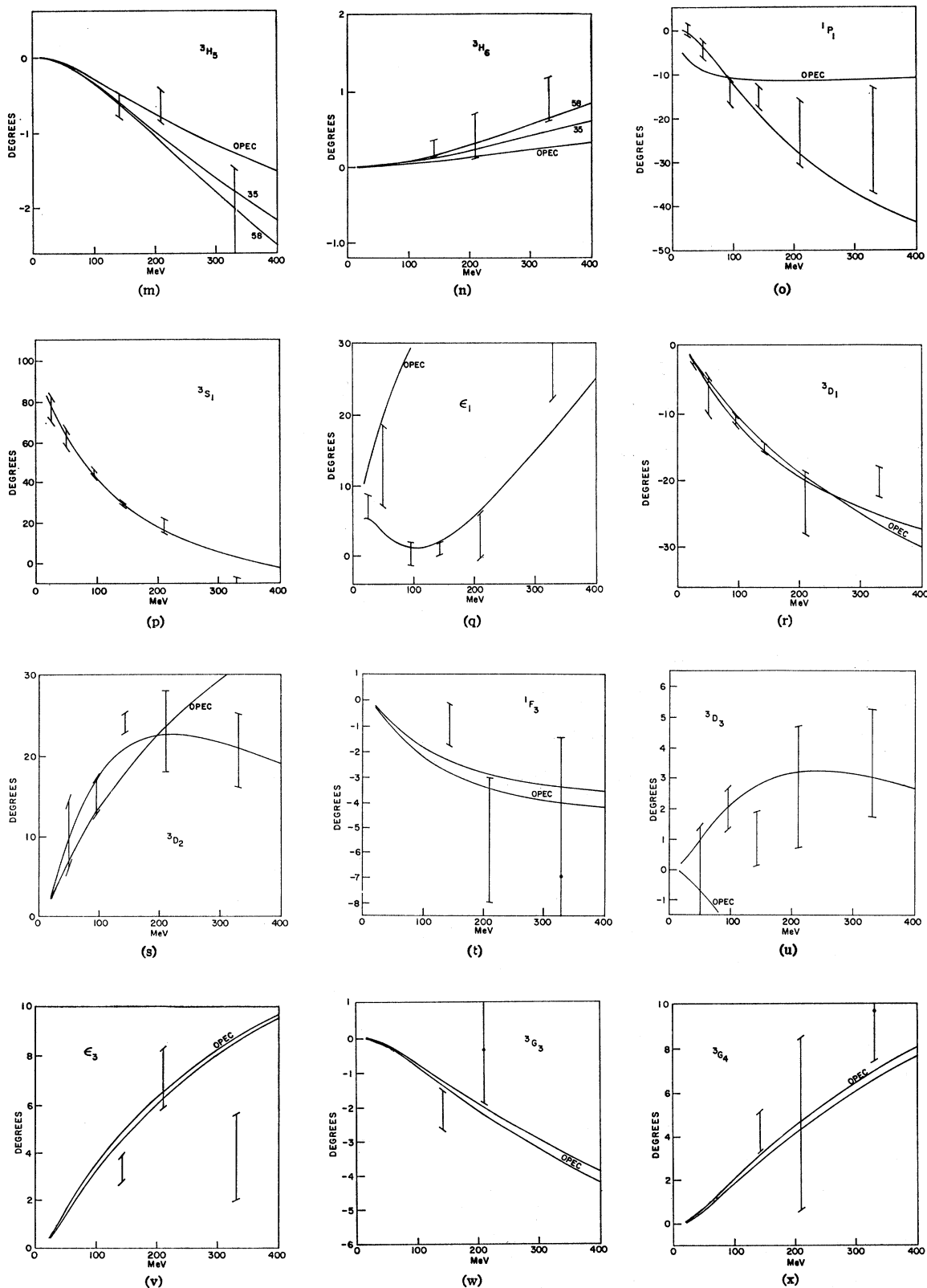


FIGURE 1 (continued).

(continued on next page.)

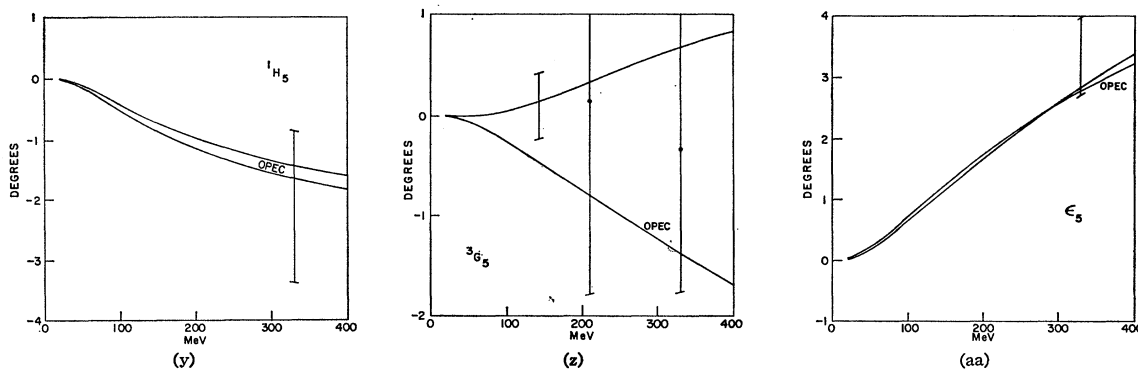


FIGURE 1 (continued).

values. In general we used as many free parameters for the EIA as the search routine would tolerate. A larger number of parameters than shown in Table VI led to a breakdown in the search procedure.

It is somewhat a matter of opinion as to whether the phase-shift values in Table V or in Table VI give the most accurate representation of the elastic-scattering matrix. In the EDA (Table V), we can use a larger number of free phase shifts than in the EIA (Table VI). This enables us to eliminate some of the errors that are caused by using OPEC to represent the higher phase shifts. We also force the data at the different energies to adjust to be consistent with one another. The price we pay is that we have imposed a particular form for the energy dependence. The best representation for the phase shifts at any one energy is of course given in Table VI. What should be stressed here is the similarity in the phase-shift values given in Tables V and VI. They are in good agreement, particularly with respect to the $T=1$ phases. Only Table VI has error bars, but these same error limits can be applied to Table V to give "corridors of errors" for the phase-shift values.

Graphical representations of our results are given in Figs. 1 and 2. Figure 1 gives the phase-shift curves for the 35- and 58-parameter EDA solutions (Table III), and also the OPEC phase-shift curve, all for $g^2=13$. Superimposed on these curves are the EIA phase-shift values with the error bars from the exact error matrix calculation (22). We can use Fig. 1 to illustrate an important point. If we examine the $T=1$ phase shifts, which are the most accurate ones from our analysis, Fig. 1 illustrates that the 1G_4 and ϵ_4 phases deviate markedly from OPEC. Hence they must be treated as free parameters in an accurate analysis. The H waves also deviate from OPEC, but the deviation is small and is about the same order of magnitude as the error limits. Hence it is not strictly necessary to include the H waves as free parameters in the EDA. However our search procedure does give good values for these phases, and including them as free parameters gives better values for the lower partial waves. Thus we have included them also. The point we are leading up to in

this discussion is that if we now consider the $T=0$ phases, the (n,p) data are not yet complete enough or accurate enough to require us to include much G -wave freedom in the phases.¹⁻³ However from the $T=1$ results, we know that the $T=0$ G waves contain significant non-OPEC contributions. Thus they should be treated as free parameters. In particular, Fig. 1 shows a strong non-OPEC behavior for the 3G_5 phase. The ϵ_5 and H_5 phases differ only slightly from OPEC, and we found that including them or not including them made a difference of less than one in χ^2 . Hence they have a negligible effect on the EDA. We have included them, since we want the EDA to have the full range of generality indicated by the $T=1$ data.

Figure 1 also illustrates the remark we have made above that the $T=1$ phases obtained from the combined analysis and from the (p,p) analysis alone are almost identical.

In Fig. 2 we have given 59- and 67-parameter EDA phase-shift values for different values of g^2 , and also the OPEC values for $g^2=13$. These curves give a good graphical representation of the stability of the solutions. The $T=1$ phases are quite stable in all cases. The $T=0$ phases, on the other hand, exhibit modest changes for the 59-parameter solution (24 free $T=0$ phases), and they exhibit fairly radical changes for the 67-parameter solution (32 free $T=0$ phases). Clearly 32 parameters represent too much freedom for the $T=0$ phases.

The EDA and EIA results are based on identical data selections, and we have made the phase-shift energy derivatives the same at each of the energy bands. Hence we should be able to use the two kinds of results to say something about the consistency of the data. To do this we can use the χ^2 breakdown for the (p,p) plus (n,p) EDA and EIA as given in Table IV. We can also use the normalization constants arrived at in the two kinds of analyses. These are given in Table VII. We draw the following conclusions about the data consistency:

At 25 MeV, the EDA and EIA χ^2 values are quite similar for the (n,p) data selections. The EDA (p,p) value of 25 is somewhat higher than the EIA value of 17. Most of the (p,p) data contribute to this increase.

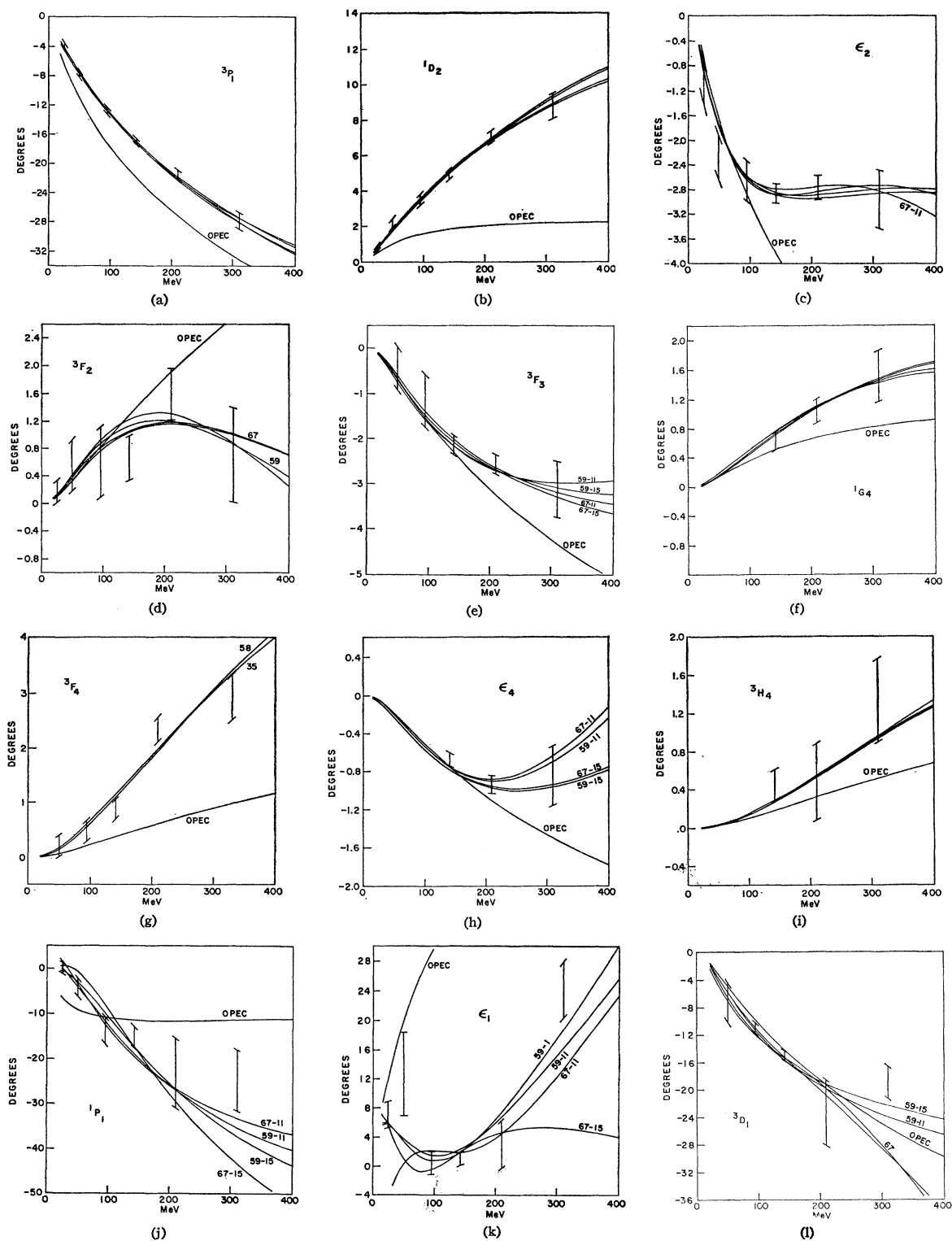


FIG. 2. Energy-dependent (p, p) plus (n, p) phase-shift solutions for 59 and 67 phase-shift parameters, with $g^2=11$ and $g^2=15$. These curves illustrate the relative stability of the $T=1$ phases and the relative instability of the $T=0$ phases, especially for 67 free parameters. Also shown are OPEC values for $g^2=13$ and error bars representing the combined EIA solutions for $g^2=13$. (These were preliminary solutions, but they illustrate the point we are attempting to establish.) The labeling on the curves follows their description here.

(continued on next page.)

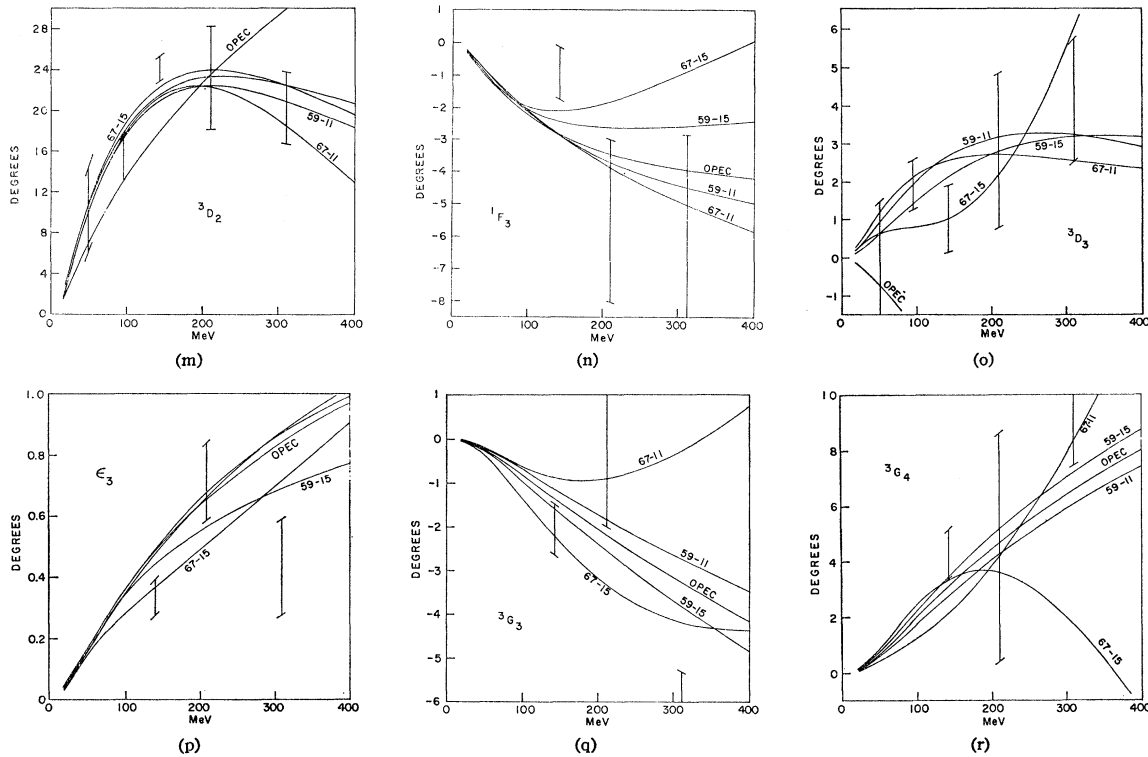


FIGURE 2 (continued).

At 50 MeV, the (p,p) χ^2 sum from the EDA (36) is considerably higher than the corresponding EIA value (22). Examination of the data shows that the EDA increase is coming from the fits to the (p,p) differential cross section and R data. In the EDA, the 51.5- and 51.8-MeV $\sigma(\theta)$ normalizations are 3 and 2% higher than the respective values arrived at in the EIA (Table VII). For the R data, the EDA normalization is 2% lower than the EIA normalization value. These are quite small differences and they illustrate the sensitivity of χ^2 to small changes in the data. Hence the (p,p) χ^2 values at 50 MeV actually indicate fairly good (p,p) data consistency there, although the results are not as consistent as at some of the other energies. The (n,p) χ^2 sum for the EDA (28) is also considerably larger than the EIA sum (18). This increase is due to both the (n,p) $\sigma(\theta)$ and P data, with about $\frac{2}{3}$ of the contributions coming from the P data. The 50-MeV (n,p) $\sigma(\theta)$ normalizations differ by less than 2% in the EDA and EIA values, but the EDA P normalization is 5% lower than the EIA normalization. Hence there may be some problem with the (n,p) $P(\theta)$ normalization at 50 MeV.

The good agreement between the EDA and EIA χ^2 values at 95 MeV, as shown in Table IV, is due to the nonrestrictiveness of the data rather than its consistency. Examination of Table VII shows that the 95 and 98 MeV (p,p) $P(\theta)$ normalizations differ by 3 and 7%, respectively, in the EDA and EIA analyses. The 95 MeV (n,p) $\sigma(\theta)$ normalizations agree to within 2%,

but the 90, 100, and 95 MeV (n,p) $P(\theta)$ normalizations differ by about 3%, with the EDA normalizations being higher in each case. The most glaring discrepancy is the fact that the 95 and 98 MeV (p,p) polarization normalizations differ from each other by about 9%. This is after we have made the necessary corrections to these data.¹⁴ Our previous analysis (III) showed only a 2% discrepancy. The corrections increase this discrepancy to 4%. The new energy dependence of the phase shifts has further increased the discrepancy. It appears that there are some inconsistencies in the (p,p) data near 95 MeV that are listed in Table VII.

The 142 MeV (p,p) and (n,p) data are generally in good agreement, as shown in Tables IV and VII. The 147 and 142 MeV (p,p) polarization measurements differ by 4% after all corrections have been included. The 143 MeV (n,p) polarization data, as listed in Table II, do not seem to be consistent with the other data. Since we have allowed the 143 MeV P data to float freely, an error in the normalization assignment would not affect the results of the present analysis. The 153 MeV (n,p) differential cross section data are responsible for the increase of 26 in the EDA χ^2 sum over the EIA χ^2 sum at 142 MeV, as shown in Table IV.

At 210 MeV, the (p,p) data are in good agreement. The increase in the (n,p) EDA χ^2 sum is due to the (n,p) differential cross section, indicating some diffi-

¹⁴O. N. Jarvis and B. Rose, AERE Harwell report (unpublished).

culty with the normalization. The (n,p) polarization data have 11% difference between the EDA and EIA normalizations, and yet χ^2 is insensitive to this difference, due to the unrestrictiveness of the (n,p) $P(\theta)$ data. This fact is reflected in the large normalization error (± 0.12) obtained from the EIA error matrix calculation.

The data we have used near 310 MeV actually range from 290 to 350 MeV. In our previous analysis (III), we quoted phase shifts at an energy of 310 MeV. In order to obtain a better midpoint energy for the matrix calculations that are described in Sec. VI, we quote the phase shifts here at an energy of 330 MeV. Tables IV and VII show that the (p,p) data in this energy band give good agreement with regard to the EDA and EIA calculations. The (n,p) data in this region, on the other hand, are very incomplete, and the normalizations are not well known. We first tried using no normalization constraint on the 350 MeV (n,p) $\sigma(\theta)$ data. We found that the (n,p) $\sigma(\theta)$ and P normalizations near 330 MeV were considerably different for the EDA and EIA. Although this has little effect on χ^2 (Table IV) it does show up in the phase shifts. We then imposed a 3% constraint, as discussed in the footnote to Table II. The $T=0$ phase shifts of Tables V and VI at 330 MeV are in only approximate agreement. In order to emphasize the approximate nature of our 330 MeV EIA $T=0$ solution, we have included the 1H_5 and ϵ_5 phases as free parameters in Table VI. Since they are close to the OPEC values anyway, their inclusion hardly affects the phase-shift values. However, the error limits are increased considerably (to more realistic values) for the $T=0$ phases. The $T=1$ phases are essentially unaffected by this change.

As a test of the validity of our phase-shift energy-dependent form (23), we calculated observables at an energy of 430 MeV and compared them against the measurements of P , D , R , A , and A' by Roth at Princeton and Chicago.¹⁵ The agreement was quite good for all of these measurements. The early MDDOP forms⁹ did not permit extrapolations to this high an energy.¹⁰ Hence our present forms are clearly an improvement.

IV. (p,p) PHASE-SHIFT ANALYSES AND CHARGE INDEPENDENCE

The entire analysis that was described in Sec. III for the combined (p,p) plus (n,p) data was repeated using just the (p,p) data selection. From our previous analyses,¹⁻³ the $T=1$ results were expected to be very similar in the two cases. Comparison of the χ^2 (p,p) columns in Table IV shows that for both the EDA and EIA, the combined and the (p,p) χ^2 values are almost identical. Hence the addition of an energy dependence to the phase-shift analysis has not altered our previous conclusion^{2,3} that charge independence is valid to a

¹⁵ R. F. Roth *et al.*, Phys. Rev. **140**, B1533 (1965).

TABLE VII. Normalization constants obtained in the energy-dependent and energy-independent phase-shift analyses. The data not listed here were not assigned normalization errors. The errors on the EIA values were obtained from the error matrix.

Energy (MeV)	Kind of datum	Renormalized values		Experimental normalization error assigned
		EDA	EIA	
25.63	(p,p) $\sigma(\theta)$	0.987	0.986 \pm 0.006	0.0093
30.0	P	1.004	1.001 \pm 0.040	0.04
27.6	R	1.018	1.001 \pm 0.029	0.03
27.6	A	1.003	1.000 \pm 0.030	0.03
27.5	(n,p) $\sigma(\theta)$	1.013	1.002 \pm 0.029	0.03
22.5	$\sigma(\theta)$	0.966	0.946 \pm 0.043	∞
23.1	P	1.003	0.999 \pm 0.017	0.017
51.5	(p,p) $\sigma(\theta)$	1.040	1.011 \pm 0.022	0.045
51.8	$\sigma(\theta)$	1.035	1.016 \pm 0.011	0.025
47.8	A	1.011	1.006 \pm 0.049	0.05
47.8	R	0.991	1.007 \pm 0.038	0.05
52.5	(n,p) $\sigma(\theta)^a$	0.991	1.007 \pm 0.016	0.017
52.5	$\sigma(\theta)^b$	0.968	0.968 \pm 0.032	0.038
50.0	P	0.930	0.982 \pm 0.041	0.048
95.0	(p,p) $\sigma(\theta)^c$	0.965	0.974 \pm 0.064	0.067
95.0	P^d	1.022	0.996 \pm 0.029	0.03
98.0	P^e	1.111	1.079 \pm 0.050	∞
99.0	(n,p) $\sigma(\theta)^a$	1.014	1.005 \pm 0.016	0.017
99.0	$\sigma(\theta)^b$	0.969	0.983 \pm 0.028	0.038
91.0	$\sigma(\theta)$	1.005	1.022 \pm 0.027	∞
90.0	P	1.060	1.028 \pm 0.040	0.051
100.0	P	0.979	0.955 \pm 0.051	0.073
95.0	P	1.087	1.052 \pm 0.046	0.08
155.0	(p,p) $\sigma(\theta)$	1.041	1.026 \pm 0.034	0.04
147	P^d	0.992	0.999 \pm 0.020	0.024
137.5	R'	0.990	1.004 \pm 0.040	0.05
139.0	A	1.036	1.042 \pm 0.032	0.04
142.0	P^e	0.950	0.961 \pm 0.024	∞
128.0	(n,p) $\sigma(\theta)$	0.987	0.992 \pm 0.017	0.022
128.0	P	0.975	0.968 \pm 0.032	0.04
130.0	$\sigma(\theta)$	1.030	1.037 \pm 0.023	0.032
137.0	$\sigma(\theta)$	1.010	1.025 \pm 0.035	0.05
140.0	P	1.015	1.007 \pm 0.029	0.044
143.0	P^d	1.135	1.153 \pm 0.030	∞
153.0	$\sigma(\theta)$	1.027	0.989 \pm 0.017	0.022
213.0	(p,p) $\sigma(\theta)$	1.016	0.985 \pm 0.040	0.042
210.0	P	0.982	0.977 \pm 0.016	0.022
217.0	P	1.022	1.012 \pm 0.018	0.022
200.0	(n,p) $\sigma(\theta)$	0.968	1.003 \pm 0.021	0.021
215.0	P	0.962	1.076 \pm 0.140	0.12
345.0	(p,p) $\sigma(\theta)^b$	0.933	0.947 \pm 0.037	0.05
345.0	$\sigma(\theta)^a$	1.005	1.013 \pm 0.035	0.05
330.0	$\sigma(\theta)$	0.965	0.967 \pm 0.048	∞
315.0	P	1.014	1.012 \pm 0.037	0.04
310.0	P	0.998	0.991 \pm 0.037	0.04
300.0	(n,p) $\sigma(\theta)$	1.065	1.036 \pm 0.041	0.1
290.0	$\sigma(\theta)$	1.071	1.054 \pm 0.081	0.1
350.0	$\sigma(\theta)$	0.994	0.982 \pm 0.027	0.1
310.0	P	0.966	0.996 \pm 0.040	0.04

^a Small-angle data points.

^b Large-angle data points.

^c These data have been multiplied by the factor 0.946 (see III).

^d These data have been multiplied by the factor 0.933 (see Ref. 14).

^e These data have been multiplied by the factor 0.911 (see Table II and Ref. 14).

high degree of accuracy over the energy range from 25 to 350 MeV.

Our conclusions about charge independence may of course arise in part because of the fact that there are as yet few kinds of (n,p) data to fit. However at 142 MeV, where the (n,p) data selection is most complete (Table I), the χ^2 (p,p) values for the combined and the (p,p) analyses vary by less than 10% for both EDA and EIA, as shown in Table IV, and in fact the EDA and

EIA differences are in opposite directions. What we would like to do would be to obtain the $T=0$ and $T=1$ scattering matrices by analyzing just (n,p) data alone. But, as we have shown,¹ such an analysis is not yet possible.

In Fig. 1 the combined and the (p,p) EDA phase-shift curves are both included. As can be seen, the agreement is very close. We have not included values for the (p,p) phases in the present paper. Values are given in Papers I–III. It has been speculated¹⁶ that the 1S_0 phase shift might exhibit observable charge-dependent effects. However, our results indicate that this speculation is not borne out experimentally.

Other investigations, in particular those of Breit and his co-workers at Yale,¹² have already established that charge independence is a valid concept in the 10–300-MeV energy region. We feel that Table IV of the present paper is the most quantitative way in which to evaluate the accuracy of the charge independence hypothesis. Examination of the phase shifts is another way of testing this hypothesis. These comparisons have been listed in Papers I–III. Still a third way is to compare the value obtained for the g^2 of the pion-nucleon coupling constant, from a modified phase-shift analysis using first (p,p) and then combined data selections. This comparison is discussed in the next section.

V. DETERMINATION OF THE PION-NUCLEON COUPLING CONSTANT

In our previous Papers I–III of this series, we have discussed the problem of obtaining a value for the pion-nucleon coupling constant via the modified phase-shift analysis. Table VII of Paper I and Table IX of Paper II show our energy-independent determinations at 95, 142, 210, and 310 MeV. At 25 and 50 MeV, we were unable to obtain a determination of g^2 , as was discussed in Paper III. Although there is a considerable spread in the g^2 values we obtained, depending on the data selection and the choice of free phase shifts, our most reliable values fell in the range from $g^2=11$ to $g^2=15$.

In our present work, we can use all of the data at once in the EDA to obtain a value for g^2 . This has several advantages. By using data at several energies, small systematic data errors should tend to cancel out. Also, the EDA permits us to use more free parameters at each energy than is possible with the EIA and yet

still maintain enough of the OPEC amplitudes in the higher phases to give a well-defined value for g^2 . Finally, we can choose our phase-shift energy-dependent forms so that the free phase-shift deviations from OPEC have the singularity structure required by the Mandelstam representation. The phase-shift energy-dependent form we used (23) has the correct singularity structure. It is also linear in the parameters p that are used in the search procedure, a fact that has computational advantages.

The g^2 determinations we obtained from the EDA are listed in Table VIII. The value $g^2=13.8\pm 1.9$, obtained using just the (p,p) data with 35 free parameters, is probably the most reliable value from the present work. The values from the combined searches are based on (n,p) data sets that are incomplete and that do not have the accuracy of the (p,p) data sets. However, the values we obtain using the combined (p,p) plus (n,p) data selection are reasonable ones and agree within error limits with the (p,p) value. This agreement is another argument in favor of the validity of the charge independence hypothesis. Table VIII also shows that there is no strong discrepancy between the value for g^2 obtained from nucleon-nucleon scattering and the value for g^2 obtained from pion-nucleon scattering ($g^2\approx 15$). This is a powerful argument in favor of the general concepts of field theory as exemplified in the use of Feynman diagrams to make dynamical calculations.

Differences in the charged and neutral pion masses lead us to expect a difference of about 0.6 in g^2 between the (p,p) and combined analyses, with the (p,p) plus (n,p) averaged g^2 having the lower value. This is about the difference we observe in Table VIII. Professor Breit and his group also obtained a similar difference (Table XI of Paper II).

VI. REDUCED SECOND-DERIVATIVE MATRICES

In this section we discuss the use of matrix methods in obtaining model fits to the nucleon-nucleon data. In particular, we consider the problem where a potential model or other theoretical form is used to calculate a portion of the scattering amplitude, and then the remaining part of the amplitude is adjusted so as to give the best fit to the experimental data. In Sec. II we considered a specific example. There we had a “model,” the phase-shift forms (23), which gave the phase shifts but not the data normalizations. We can envision other models in which, for example, the $l=1$ and higher phase shifts are given from theory, but the S waves must be treated phenomenologically.

Our starting point is Eq. (1). This gives χ^2 as a function of the set of phase shifts δ and the set of normalization constants α . Now suppose we have a theoretical model that predicts values for a set m taken from (δ,α) and does not give values for the remaining parameters n . We can write

$$\chi^2 = \chi^2(\delta,\alpha) = \chi^2(m,n), \quad (25)$$

TABLE VIII. Values for the pion-nucleon coupling constant g^2 obtained from the present energy-dependent phase-shift analyses.

Data selection	Free parameters	g^2
(p,p)	35	13.8 ± 1.9
(p,p)	24	13.9 ± 1.0
(p,p) plus (n,p)	58	13.1 ± 0.8
(p,p) plus (n,p)	66	13.4 ± 0.7

¹⁶ P. Signell, Phys. Letters 8, 73 (1964).

where a vector notation is understood for δ, α, m , and n . The vector m will in general depend on a set of model parameters that are to be adjusted so as to minimize χ^2 . At the minimum we have

$$\chi_0^2 \equiv \chi^2(m_0, n_0). \quad (26)$$

Let

$$\Delta m \equiv m - m_0, \quad \Delta n \equiv n - n_0. \quad (27)$$

Then in matrix notation

$$\chi^2(m, n) = \chi_0^2 + (\Delta m, \Delta n) \begin{bmatrix} A & B \\ \bar{B} & C \end{bmatrix} \begin{bmatrix} \Delta m \\ \Delta n \end{bmatrix}, \quad (28)$$

where

$$\begin{aligned} A_{jk} &= - \left. \frac{\partial^2 \chi^2}{2 \partial m_j \partial m_k} \right|_{m_0}, \\ B_{jk} &= - \left. \frac{\partial^2 \chi^2}{2 \partial m_j \partial n_k} \right|_{m_0, n_0}, \\ C_{jk} &= - \left. \frac{\partial^2 \chi^2}{2 \partial n_j \partial n_k} \right|_{n_0}. \end{aligned} \quad (29)$$

Given the vector Δm , we wish to minimize χ^2 by adjusting the vector Δn . Setting

$$\partial \chi^2 / \partial \Delta n = 0 \quad (30)$$

in (28), we obtain

$$\Delta n_{\min} = -C^{-1} \bar{B} \Delta m. \quad (31)$$

Substituting (31) into (28), we have finally

$$\chi^2 = \chi_0^2 + \widetilde{\Delta m} (A - BC^{-1} \bar{B}) \Delta m. \quad (32)$$

Let

$$R \equiv A - BC^{-1} \bar{B} \quad (33)$$

be denoted as the *reduced second-derivative matrix*.

Once the phase-shift analysis has been completed, we know the values (m_0, n_0) or (p_0, α_0) , also the value for χ_0 , and then we can calculate the matrices A, B, C . Then if we are given a theoretical model that predicts the values Δm , we can form the matrix R having the proper dimensionality, and the equation

$$\chi^2 = \chi_0^2 + \widetilde{\Delta m} R \Delta m \quad (34)$$

will give the least-squares-sum χ^2 to the data predicted by the model, with all free parameters (the Δn) adjusted to obtain the best fit. Also, Eq. (31) will give the values for the Δn . Hence if the model predicts P waves and higher, (31) will give the value for the S waves arrived at by fitting the data.

If a theoretical model gives phase shifts δ in terms of a *linear* set of parameters p , then the reduced second-derivative matrix can be used directly to give the values for p that minimize χ^2 , with no search being required. To show this, consider the model phase shifts $\delta^m(p)$. From the phase-shift analysis we have the phases δ_{exp}^m . Thus

$$\Delta \delta^m = \delta^m(p) - \delta_{\text{exp}}^m \quad (35)$$

and

$$\Delta \delta^m = \Delta \delta^m(p_0) + [\nabla_p \cdot \Delta \delta^m(p)] \Delta p \quad (36)$$

in our (understood) vector notation, where p_0 is any initial set of parameters p . Substituting in (34), and using

$$D \equiv \nabla_p \cdot \delta^m(p), \quad \Delta_0 \equiv \Delta \sigma^m(p_0), \quad (37)$$

we have

$$\chi^2 - \chi_0^2 = \Delta \chi^2 = (\Delta_0 + D \Delta p) R (\Delta_0 + D \Delta p). \quad (38)$$

Taking

$$d \Delta \chi^2 / d \Delta p = 0 \quad (39)$$

gives

$$V \Delta p = -W, \quad (40)$$

where

$$V \equiv \bar{D} R D, \quad W \equiv \bar{D} R \Delta_0. \quad (41)$$

Hence *any* initial set of parameters p will specify the vector Δ_0 , and (40) will give Δp leading to the minimum simply by a process of matrix inversion.

As a test of these ideas, we chose the theoretical forms (23) as a "model," obtained the matrices A, B , and C (29) from the EIA (p, p) and combined analyses (21) and (22), and solved for the parameters p_j (23) using a sum over energies for (29), (33), (38), (40), and (41). The results of this calculation are shown in Table IX. The first two data columns give the phase-shift solution results. The third column gives the $\Delta \chi^2$ (38) predicted by the reduced second-derivative matrix R (33) and (34) at each energy. The fourth column gives the $\Delta \chi^2$ ob-

TABLE IX. Comparison of χ^2 values obtained by fitting the data and by fitting the reduced second-derivative matrix.

Energy band (MeV)	(p, p) data selection						Combined data selection			
	χ_0^2	$\Delta \chi_0^2$	$\Delta \chi_R^2$	$\Delta \chi_R^2$	$\Delta \chi_D^2$	$\Delta \chi_D^2$	χ_0^2	$\Delta \chi_0^2$	$\Delta \chi_R^2$	$\Delta \chi_R^2$
25	16 ^a	5 ^b	5 ^c	8 ^d	7 ^e	31 ^d	29 ^a	13 ^b	16 ^c	25 ^d
50	22	10	9	9	5	54	40	24	45	24
95	38	5	4	5	5	28	136	8	9	26
142	102	9	10	10	18	44	213	26	28	27
210	28	6	5	6	5	18	53	27	24	29
330	53	5	7	13	8	75	81	12	124	201
Sum	259	40	40	51	48	250	552	110	246	329
Total χ^2		299	299	310	307	509		659	798	881

^a From EIA (Table IV).

^b Calculated from reduced second-derivative matrix.

^c Calculated from diagonal terms of reduced second-derivative matrix.

^d EDA minus EIA (Table IV).

^e Obtained from fitting the data.

tained by fitting the theoretical solution to the actual data selection, using (1). In this calculation the normalization parameters α^i were obtained from (31) and no searching was done. The χ^2 value predicted for the energy-dependent (p,p) solution obtained from (40) is 299, and the actual value obtained from (1) for this solution is 310. The exact solution gives 299. Thus for all practical purposes, the reduced second-derivative matrix R is equivalent to the actual (p,p) data selection in making fits to theoretical models.

As a further test of these ideas, we obtained a theoretical solution by taking only the diagonal elements of R , and hence neglecting all correlations. This solution predicted a (p,p) χ^2 value of 307. However, a fit against the data gave a χ^2 value of 509. Thus the effect of ignoring correlations is to raise χ^2 by about 200 for our (p,p) data selection. When theoretical models are fit against phase shifts, the solution $\Delta\chi_D^2$ is what is actually being obtained. Hence a model that gives a value χ_m^2 in fitting a complete set of (p,p) phase shifts (say the $T=1$ phases shown in Table VI), will give a value $\chi^2 \approx \chi_m^2 + 259 + 200$ when tested against our (p,p) data selection.

This same calculation was repeated for the combined analysis, as shown in Table IX. With $\chi_0^2 = 552$ from the sum of the EIA, the solution obtained by fitting the reduced second-derivative matrix was calculated to have $\chi^2 = 798$, and a direct fit against the data gave $\chi^2 = 881$. These values are considerably higher than the EDA value of 662 from the phase-shift search. Essentially all of this increase comes from the (n,p) data in the 330-MeV energy band. The (n,p) data here are very incomplete, and they occur at energies of 290, 300, 310, and 350 MeV. It is not surprising that a second-derivative matrix calculated at 330 MeV is not very accurate when extrapolated up 20 MeV and down 40 MeV. The two smallest angle cross-section points at 350 MeV contribute 156 to χ^2 for the theoretical solution based on a fit to R . Thus the method of fitting the reduced second-derivative matrix must be used with some caution when fitting (n,p) data, especially when these data lie on the extremes of the energy range under consideration. At the extremes, the phase-shift derivatives are not well determined. Even for the excellent (p,p) fit using R , the worst results occur at 330 MeV, as shown in Table IX.

VII. CONCLUSIONS

The nucleon-nucleon elastic-scattering data are now complete enough that the scattering matrices are quite well defined over the entire energy region up to around 350 MeV. Improvements in the data will continue to be made, but the qualitative features of the scattering are not likely to be altered by these changes. We feel that in this paper the modified phase-shift analysis has been used so as to extract the maximum amount of information from the existing experimental data in the

energy ranges under consideration. The theoretical form we have used to represent the phase shifts should be considered as a forerunner to a more exact dispersion-theoretic treatment. We have not investigated in detail the dependence of our phase-shift results on the form used, but we did some checking with forms having a different singularity structure. The results were essentially the same as the one we quote here.

Trying to use the experimental results to establish the "correct" form for the phase-shift energy dependence is a most formidable task. The accuracy of the present data clearly do not warrant such an attempt. In the dispersion theory approach,¹¹ which is currently fashionable, we need an accurate knowledge of the scattering matrix above the inelastic threshold to describe scattering in the energy region below the threshold. Phase-shift analyses have been made at energies above 400 MeV.¹⁷ Comparison of our results with these analyses and with the work of Roth¹⁵ shows that the real parts of the phase shifts exhibit a smooth energy dependence in going above the inelastic threshold. The experiments above 400 MeV are not yet complete enough to permit accurate determination of the imaginary parts of the phase shifts. Theoretical work on this problem is still rudimentary and is based mainly on the dominance of the (3,3) final-state interaction.

Note added in proof. Very recently three 25-MeV correlation measurements have been carried out. These include $C_{NN}(90^\circ)$ and $A_{XX}(90^\circ)$ for (p,p) scattering at 25.7 MeV [J. Thirion, Saclay (private communication)], and $C_{NN}(175^\circ)$ for (n,p) scattering at 23 MeV [J. Simmons, Los Alamos, preliminary data (private communication)]. We found that adding the two (p,p) data points shifted all of the $T=1$ phases at 25 MeV by a standard deviation or more. Adding the (n,p) datum changed ϵ_1 from $+7^\circ \pm 2^\circ$ to $-4^\circ \pm 2^\circ$. These changes illustrate the fact that the data sets at some energies are not yet complete, as we have tried to emphasize in our discussions, and the error limits as given by the error matrix should be viewed skeptically at these energies. In particular, the anomalous behavior of ϵ_1 at 25 and 50 MeV is due to the paucity of (n,p) data at these energies, as was indicated in Paper III of this series. These 25-MeV results were reported on by H. P. Noyes [International Conference of Polarization Phenomena Off Nucleons, Karlsruhe, 1965 (unpublished)].

ACKNOWLEDGMENTS

We would like to thank Robert Wright for assistance with the data collection. Thanks are also due to Sidney Fernbach, who has given interest and encouragement to this work during the many years that it has evolved at Livermore.

¹⁷ For example, Y. Hama and N. Hoshizaki, *Progr. Theoret. Phys. (Kyoto)* **31**, 609 (1964); L. S. Ashgirey, N. P. Klepikov, Ya. P. Kumekin, M. G. Mescheryakov, S. B. Nurushhev, and G. D. Stoletov, *Phys. Letters* **6**, 196 (1963).